Two-dimensional LNA/DNA arrays: estimating the helicity of LNA/DNA hybrid duplex†

Sherri Rinker, Yan Liu and Hao Yan*

Received (in Austin, TX, USA) 14th March 2006, Accepted 24th April 2006
First published as an Advance Article on the web 23rd May 2006
DOI: 10.1039/b603872g

We measured the helical repeats of a non-natural nucleic acid, locked nucleic acid (LNA), by incorporating LNA strands into the outer arms of a DNA double crossover (DX) molecule; atomic force microscopy (AFM) imaging of the two-dimensional (2D) arrays self-assembled from these DX molecules allows us to derive the helical repeat of the LNA/DNA hetero-duplex to be 13.2 ± 0.9 base pairs per turn.

Self-assembly of branched DNA nanostructures into extended structures with sub-nanometer dimensional precision has recently attracted much attention.[1–3] A variety of one-dimensional (1D) and 2D periodic arrays[4–7] and tubes[8–10] have been constructed. These DNA nanostructures can possibly be used as templates for assembly of nanoelectronic components.[11–14] To achieve more robust self-assembling DNA nanoarrays, high thermal stability of both DNA building blocks and the arrays is very desirable.

Locked nucleic acid is a nucleic acid analog in which the ribose ring is constrained (locked) by a methylene linkage between the 2′-oxygen and the 4′-carbon.[15] LNA hybridizes with DNA and RNA through Watson–Crick base pairing and the hybrid duplexes display unprecedented thermal stabilities as compared to unmodified DNA/DNA and DNA/RNA duplexes.[16] Melting temperature increases ranging from 0.2 to 8 °C per LNA base have been reported,[17,18] depending on the oligomers' length, sequence and number of LNA bases in the oligomers. The increased thermal stability is proposed to be due to the bridge conformation in the LNA bases that reduces the conformational flexibility of the ribose and increases the local organization of the phosphate backbone.[18,19] LNA oligos are as soluble as DNA and RNA, they can be obtained using standard reagents and automated synthesis, and can be purified and analyzed using the same methods employed for standard DNA. These all make LNA an attractive candidate to be used in nucleic acids nanotechnology as building blocks for scaffolding templates.

In the design and assembly of constructs including LNA bases, we need to take into account the structural differences between LNA and DNA, that is the geometry of the hybrid duplex, especially the helical repeating unit. Structural analysis by NMR and X-ray have shown that a LNA/RNA hybrid adopts an almost canonical A-type duplex morphology, with an average twist angle between the base-pairs of 29.6°,[16,20] corresponding to ~12 bp per whole helical turn. LNA/DNA hybrid structurally reassembles a RNA/DNA hybrid, and the B-type character of the duplexes decreases and A-type character increases as an increased number of LNA monomers are incorporated.[16] Compared with a DNA duplex, a LNA/DNA duplex shows an unwinding of the helix and widening of the minor groove.[21] Despite substantial studies by solution NMR,[19,21–23] the helical repeat of LNA/DNA duplexes is still not well known.

Recently Seeman and coworkers[24] developed a method to estimate the helicity of a PNA/DNA duplex by incorporating PNA sequences into a DNA tile to examine the formation of 2D arrays using a two-DX tile system. Here we employed the same method and utilized the AB* system[24,25] to measure the helical repeat of a LNA/DNA hetero-duplex (see ref. 24 for detailed description of definition of the AB* tiles). Briefly, the DX tile (A) and a DX + J tile (B*),[25] each of which is equipped with sticky ends that are designed to associate with the other tile but not with itself. When the A and B* tiles are mixed, two-dimensional planar arrays can form when the two distances between the intermolecular crossovers are an odd number of helical turns. Otherwise, linear arrays or random aggregates can form but not a 2D array. The 2D arrays display the hairpins on the B* tiles as stripes when imaged by AFM, with a spacing of 32 nm (9 full turns between the center of two B* tiles).

In this design, two versions of the A tile were assembled, AD, which is entirely DNA and AL where the two short crossover strands (colored red) consist of LNA (Fig. 1). Nine versions of the B* tile were assembled, B0–B8; the numeral indicates the number of different nucleotide pairs added to compensate for the expected twist when AL is incorporated into the arrays.

We used AFM to monitor the formation of arrays that included all combinations of the tiles (Fig. 2). The AD tile consists of DNA only, forms arrays cleanly with tiles B0 and B1, as expected. As the number of added bases increases, the self-assembly fails, and random aggregates or short linear arrays (200–500 nm) are obtained. In contrast, the corresponding arrays combining the AL tile with B0, B1, B2 are ill-formed. However, combining the AL tile with B3, B4 and (to some extent) B5 leads to well-patterned arrays; these arrays display stripes with the expected 33 nm periodicity (B3 is 1 nm longer than B0). The remaining combinations do not form 2D arrays, but rather random aggregates similar to the AD/B2 to AD/B8. These data demonstrate the incorporation of LNA oligomers into a nucleic acid nanostructure capable of forming ordered 2D arrays.

For the extended 2D arrays to be able to form, each of the four arms of the AL and B3 (or B4) tiles that are connected through the complementary sticky ends is necessary to be 2.5 helical turns. The

Department of Chemistry & Biochemistry and Biodesign Institute, Arizona State University, Tempe, AZ 85287, USA. E-mail: hao.yan@asu.edu; Fax: (+1) 480 727 2378; Tel: (+1) 480-727-8570

† Electronic supplementary information (ESI) available: Experimental methods and DNA sequences. See DOI: 10.1039/b603872g

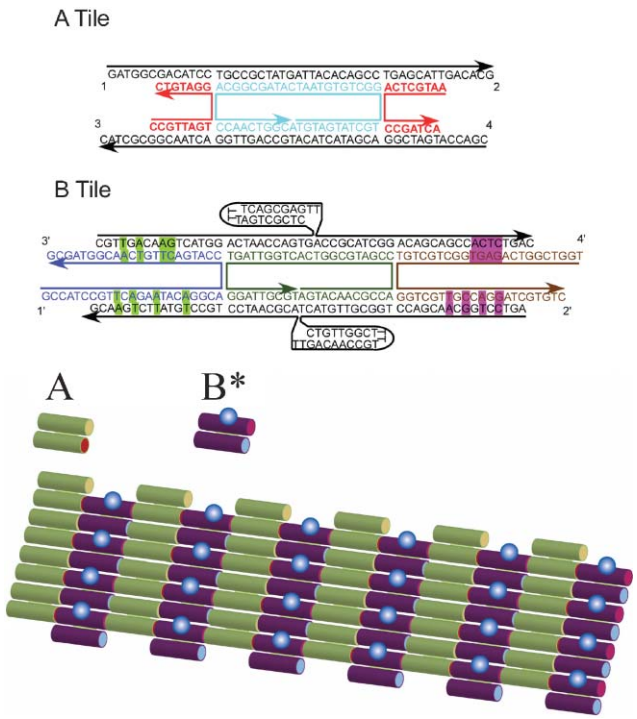

Fig. 1 The DX tiles used in this study. The upper tile is the A tile: in AD the two strands in red consist of DNA whereas in AL they consist of LNA (see text for definition of AD and AL). The lower tile is the B8 tile. Base pairs are added alternately to the left and right pairs of outer arms to form tiles B1–B8 as shown by the pink and green highlights: *e.g.* to form B1 from B0, a base pair is added to both pink regions; to form B2 from B1, a base pair is added to both green regions. Complementary sticky ends are shown as numbers. The lower part of the figure shows the tiles forming a two dimensional array.

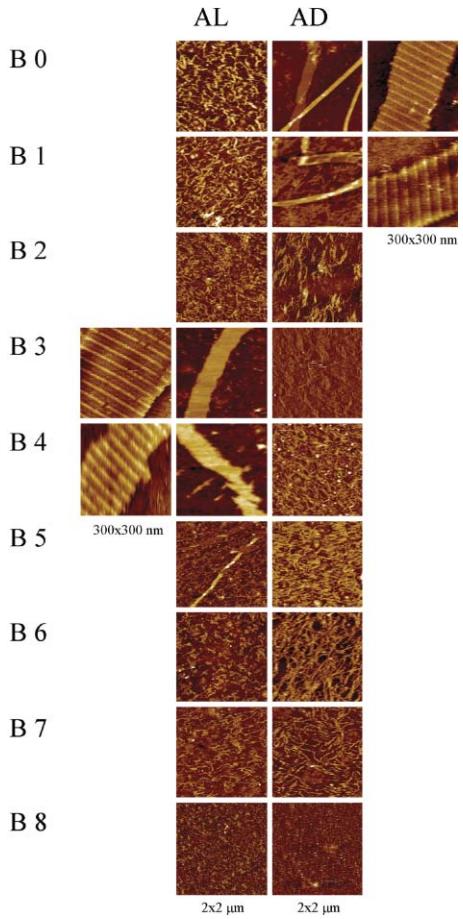

Fig. 2 AFM images of arrays formed from the tiles AL and AD with tiles B0–B8. The images in the two columns are of a 2000 nm field and the height scale ~6.0 nm. AL/B3, AL/B4, AD/B0 and AD/B1 have zoomed images (scan scale ~300 nm) on the left and right, respectively, showing the periodic features of the arrays.

helical repeat of the DNA/LNA segment of AL can be calculated assuming that the average helical repeat for the rest of the system remains at 10.5 base pairs per helical turn (bp/t). The lengths of the four arms in the AL/B3 and AL/B4 systems correspond to an average helical repeat of 13.2 bp/t with a standard deviation of $\pm$0.9 bp/t for the LNA/DNA hybrid duplexes. This is measured over the 30 DNA/LNA base pairs present per tile. This number is consistent with the results obtained by the solution NMR studies showing slight un-twisting of the helices based on 9 bp LNA/DNA hybrid duplexes containing three to nine LNA bases. Compared to the other unnatural nucleic acid peptide nucleic acids (PNA) that have an uncharged backbone, the LNA/DNA hybrid shows tighter twisting of the helix than the PNA/DNA hybrid as measured using the same method.[24]

Melting temperature was measured for the AD tile and AL tile (Fig. 3A and B). Both tiles show two distinct thermal transitions, 59 °C and 69 °C for the AL tile, and 53 °C and 68 °C for the AD tile. The higher temperature transition for the AD and AL tiles occur at the same temperature, whereas the lower temperature transition is 6 °C higher for the AL tile than the AD tile. In order to assign the thermal transitions in the AL and AD tiles, we also obtained melting curves for partial complexes of the tiles shown from Fig. 3C to 3F.

First, to test the melting of the outer arms of the AD or AL we hybridized a 15 base DNA to a 7 base DNA strand and a 15 base LNA to a 7 base DNA as shown in Fig. 3C and 3D, respectively. The melting curves show a transition at 32 °C for the DNA/DNA pair and 57 °C for the LNA/DNA pair. It is noted that the melting of the LNA/DNA pair is close to the low temperature transition for the complete AL tile at 59 °C. There is a 25 °C increase in melting temperature over 7 LNA/DNA base pairs, corresponding to ~3.5 °C per LNA base. Second, a partial tile containing three strands that omit the two 15 base DNA or LNA strands on the ends of the tile shows two melting transitions at 49 °C and 67 °C (Fig. 3E). This is because the nick point of the center strand makes the two helices unequal, 21 undisrupted base pairs in one helix and 11 or 10 base pairs in the other. Thus two thermal transitions are observed. Third, the two-strand complex with 11 and 10 base pairs show only one transition at 49 °C (Fig. 3F), the same as the low temperature transition for the three-strand complex. Therefore the high temperature transition in the AD and AL tile was assigned unambiguously to the longest undisrupted DNA duplex in both of the tile structures that contains 21 DNA/DNA base pairs. It is interesting to note that, in comparison with the three-strand complex, incorporation of the two 15-based DNA in the complete AD tile makes the tile more stable with a 4 °C increase in the lower temperature transition, while incorporation of the two 15-based LNA strands makes the tile even more stable with a ~10 °C increase in that transition.

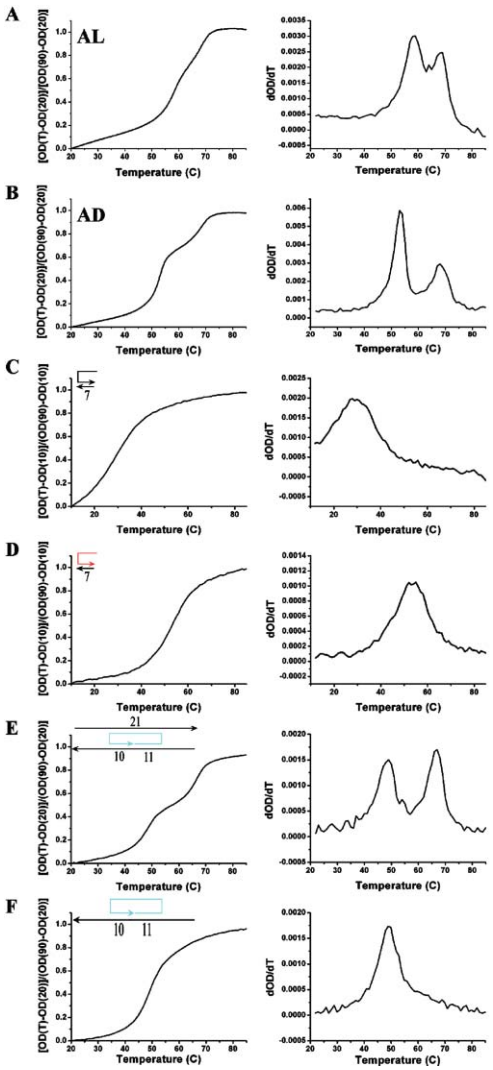

Fig. 3 The melting curves, the temperature dependence of the relative absorbance change expressed in [OD(T)-OD(20)]/[OD(90)-OD(20)] and the derivative of the melting curves are shown side by side. (A) AL tile, (B) AD tile, (C) a DNA(15)/DNA(7) complex, (D) a LNA(15)/DNA(7) complex, (E) three strand complex, (F) two strand complex. The number of base-pairing between the strands are labeled on the figure.

The change in the tile melting temperature also makes an observable difference in the 2D tile arrays formed. The AFM images for a large scan area consistently show ribbons or tubes in the width range from 50 nm to 250 nm for the AD/B0 sample, while for the AL/B3 sample no tubes were observed, but rather wider ribbons in the range of 200–500 nm were formed. Based on the understanding of the mechanism of DNA tube formation, DNA nanotubes are thermodynamically allowed, because for a 2D sheet to wrap up into a tube, the free energy of the unpaired sticky ends is minimized. But whether or not a DNA tube can form is a kinetically controlled process as there is a competition between the array wrapping up into a tube as the two opposite edges of a sheet find each other and the array growing into a size large enough that reduces the chance of the tube formation.[26] The higher melting temperature of the tiles in AL makes the tile formation and array formation (with melting temperature ~40 °C) more separated in temperature and thus more separated in time during the annealing process. Therefore the tile arrays in the case of the AL/B3 system experience a longer growth phase, they can grow wider.

We have demonstrated that it is possible to replace DNA strands with LNA strands in the formation of 2D nucleic acid arrays. With the helical properties known, the design of various DNA nanostructures can be easily modified to incorporate the non-natural nucleic acids to form hetero-polymeric arrays. The rich functional possibilities of unnatural oligomeric variants of DNA molecules can be utilized in structural nucleic acid nanotechnology.

This research has been supported by grants CCF-0453685, CCF-0453686 and a Career award CTS-0545652 from NSF.

Notes and references

1 N. C. Seeman, *Trends Biochem. Sci.*, 2005, **30**, 119–125.
2 H. Yan, *Science*, 2004, **306**, 2048–2049.
3 U. Feldkamp and C. M. Niemeyer, *Angew. Chem., Int. Ed.*, 2006, **45**, 1856–1876.
4 E. Winfree, F. R. Liu, L. A. Wenzler and N. C. Seeman, *Nature*, 1998, **394**, 539–544.
5 H. Yan, S. H. Park, G. Finkelstein, J. H. Reif and T. H. LaBean, *Science*, 2003, **301**, 1882–1884.
6 Y. Liu, Y. G. Ke and H. Yan, *J. Am. Chem. Soc.*, 2005, **127**, 17140–17141.
7 Y. He, Y. Chen, H. P. Liu, A. E. Ribbe and C. D. Mao, *J. Am. Chem. Soc.*, 2005, **127**, 12202–12203.
8 P. W. K. Rothemund, A. Ekani-Nkodo, N. Papadakis, A. Kumar, D. K. Fygenson and E. Winfree, *J. Am. Chem. Soc.*, 2004, **126**, 16344–16352.
9 J. C. Mitchell, J. R. Harris, J. Malo, J. Bath and A. J. Turberfield, *J. Am. Chem. Soc.*, 2004, **126**, 16342–16343.
10 F. Mathieu, S. Liao, J. Kopatsch, T. Wang and N. C. Seeman, *Nano Lett.*, 2005, **5**, 661–665.
11 J. Sharma, R. Chhabra, Y. Liu, Y. G. Ke and H. Yan, *Angew. Chem., Int. Ed.*, 2006, **45**, 730–735.
12 J. P. Zhang, Y. Liu, Y. G. Ke and H. Yan, *Nano Lett.*, 2006, **6**, 248–251.
13 Z. X. Deng and C. D. Mao, *Nano Lett.*, 2003, **3**, 1545–1548.
14 J. D. Le, Y. Pinto, N. C. Seeman, K. Musier-Forsyth, T. A. Taton and R. A. Kiehl, *Nano Lett.*, 2004, **4**, 2343–2346.
15 J. Wengel, A. Koshkin, S. K. Singh, P. Nielsen, M. Meldgaard, V. K. Rajwanshi, R. Kumar, J. Skouv, C. B. Nielsen, J. P. Jacobsen, N. Jacobsen and C. E. Olsen, *Nucleosides, Nucleotides Nucleic Acids*, 1999, **18**, 1365–1370.
16 B. Vester and J. Wengel, *Biochemistry*, 2004, **43**, 13233–13241.
17 P. M. McTigue, R. J. Peterson and J. D. Kahn, *Biochemistry*, 2004, **43**, 5388–5405.
18 D. A. Braasch and D. R. Corey, *Chem. Biol.*, 2001, **8**, 1–7.
19 M. Petersen, C. B. Nielsen, K. E. Nielsen, G. A. Jensen, K. Bondensgaard, S. K. Singh, V. K. Rajwanshi, A. A. Koshkin, B. M. Dahl, J. Wengel and J. P. Jacobsen, *J. Mol. Recognit.*, 2000, **13**, 44–53.
20 K. E. Nielsen, J. Rasmussen, R. Kumar, J. Wengel, J. P. Jacobsen and M. Petersen, *Bioconjugate Chem.*, 2004, **15**, 449–457.
21 G. A. Jensen, S. K. Singh, R. Kumar, J. Wengel and J. P. Jacobsen, *J. Chem. Soc., Perkin Trans. 2*, 2001, 1224–1232.
22 M. Petersen, K. Bondensgaard, J. Wengel and J. P. Jacobsen, *J. Am. Chem. Soc.*, 2002, **124**, 5974–5982.
23 K. E. Nielsen, S. K. Singh, J. Wengel and J. P. Jacobsen, *Bioconjugate Chem.*, 2000, **11**, 228–238.
24 P. S. Lukeman, A. C. Mittal and N. C. Seeman, *Chem. Commun.*, 2004, 1694–1695.
25 F. R. Liu, R. J. Sha and N. C. Seeman, *J. Am. Chem. Soc.*, 1999, **121**, 917–922.
26 Y. G. Ke, Y. Liu, J. P. Zhang and H. Yan, *J. Am. Chem. Soc.*, 2006, **128**, 4414.